Catalysis Today 139 (2008) 49–58

Contents lists available at ScienceDirect

Catalysis Today

journal homepage: www.elsevier.com/locate/cattod

Mechanism of selective catalytic reduction of NO over Ag/Al_2O_3 with the aid of non-thermal plasma

Junhua Li *, Rui Ke, Wei Li, Jiming Hao

Department of Environment Science and Engineering, Tsinghua University, Beijing, China

ARTICLE INFO

Article history:
Available online 21 September 2008

Keywords:
Non-thermal plasma
Selective catalytic reduction
Lean burn
NO_x
NTP-assisted catalysis
$Ag/\gamma\text{-}Al_2O_3$
Propene
In situ diffuse reflectance FT-IR spectroscopy (DRIFTS)

ABSTRACT

The mechanism of selective catalytic reduction (SCR) of NO by propene over Ag/Al_2O_3 was investigated with the aid of non-thermal plasma (NTP) using in situ diffuse reflectance infrared Fourier transform spectroscopy (DRIFTS). The HC-SCR reactions were proposed to be divided into two main processes, viz. nitration and reduction, which were aimed to generate isocyanate species (–NCO) and reduce NO_x, respectively. The nitration process of thermal HC-SCR was suggested to be effective only in presence of abundant electron-rich organic species. The efficiency of the reduction process was determined by the balance between the oxidation of isocyanate species and the reaction of isocyanate species with NO_3^-. Thermal C_3H_6-SCR was found to be ineffective below 400 °C, mainly owing to the inability of propene oxidation to provide oxygenates for nitration. With the assistance of NTP, the nitration process could be promoted by activating propene in an O-predominant or N-predominant environment to electron-rich organic oxygenates or $C_xH_yO_zN$ species (such as RCN and RNO_2, etc.), respectively. Nitrates reacts with electron-rich organic oxygenates effectively and generates isocyanate species. The $C_xH_yO_zN$ species can directly oxidized by oxygen or decomposed into isocyanate species over Ag/Al_2O_3. The lack of nitrates or the inability of nitrates to provide enough NO_2^+ in the reduction process probably leads to the low deNO_x activities in NTP-assisted C_3H_6-SCR in presence of SO_2 or at low temperatures below 250 °C.

1. Introduction

Selective catalytic reduction (SCR) of NO_x by hydrocarbons has attracted much attention as a potential means for NO_x removal in oxygen-rich conditions, since the NO_x reduction in C_3H_6-SCR over Cu-ZSM-5 was firstly reported in 1990s [1,2]. Various kinds of catalysts such as ion-exchanged zeolites, noble metals and metal oxides were extensively examined, among which Ag/Al_2O_3 is considered to be very promising for application due to its high activity [3–13]. In addition, silver catalysts have shown an even further enhancement in activity and some resistance to SO_2 for NO reduction when oxygenated hydrocarbons are used as reductants [14,15].

Concerning the mechanism of C_3H_6-SCR, NO oxidation to NO_2 by the catalysis of silver over alumina was once suggested to be the first step, however, the NO_x conversions over Ag/Al_2O_3 in the reduction of NO were similar with those over alumina in the reduction of NO_2. Current studies were inclined to separate the role of silver into metallic silver and silver ion. Ag^+ is a good catalyst for selective reduction of NO_x during which NO is most converted to absorbed nitrates while metallic silver is favorable to NO oxidation and leads to the formation of N_2O in HC-SCR [16]. The partial oxidation of hydrocarbon reductants is also proved to be important for HC-SCR. Unsaturated or higher alkanes (i.e. C_2H_4, C_3H_6, C_4H_8, C_8H_{18}) show higher activities at moderate reaction temperatures, due to their higher advantages in partial oxidation to generate oxygenate intermediates than saturated or light alkanes [17–20]. Alcohols (i.e. C_2H_5OH, CH_3OH, etc.) are also more effective than alkanes, especially in the temperature range of 250–350 °C [21]. Several intermediates, including NO_3^-, acetate, R-NO_2, R-ONO, –NCO and –CN species were observed to be closely related to the activity of HC-SCR, based on the mechanism studies by IR spectroscopy and other ways [22–26]. A conventional reaction pathway in C_3H_6-SCR over Ag/Al_2O_3 includes the oxidation of NO to ad-NO_x, partial oxidation of C_3H_6 to acetate, $NO_3^- + COO^- \rightarrow RNO_2 + RONO \rightarrow -NCO + -CN +$ ad-NO_x (or NO_x) $\rightarrow N_2$ [26], in which the IR peak at 1645 cm^{-1} is attributed to RNO_2 species. In order to explain the higher efficiency of C_2H_5OH-SCR than C_3H_6-SCR over Ag/Al_2O_3 (especially below 450 °C), Yu et al. [24] assigned the IR peaks at 1633, 1416 and 1336 cm^{-1} to enolic species and proposed that large amount of enolic species was essential for the formation of isocyanate species instead of acetate. These peaks were also observed to be strong in

---

* Corresponding author. Tel.: +86 10 62771093; fax: +86 10 62785687.
E-mail address: lijunhua@tsinghua.edu.cn (J. Li).

0920-5861/$ – see front matter © 2008 Elsevier B.V. All rights reserved.
doi:10.1016/j.cattod.2008.08.007

C_8H_{18}-SCR over Ag/Al_2O_3 at 350 °C, the decrease of which, however, promoted the deNO$_x$ activity in presence of H_2O [18]. Regarding of C_2H_5OH-SCR below 250 °C, the activities are still very low, despite the abundance of surface enolic species and nitrate species. It is also quite unclear whether the reduction of nitrate with isocyanate species is effective at such low temperatures.

Non-thermal plasma (NTP), with remarkably oxidizing ability, is appropriate for NO oxidation and hydrocarbons activation. Using NTP to assist HC-SCR has shown its value in application especially at low space velocity [27–36]. The activities of HC-SCR over metal oxide catalysts (Al_2O_3) were found to be effectively promoted above 250 °C with the assistance of NTP [27–30]. The effective reaction temperature could be further extended below 200 °C, if zeolite-based catalysts (i.e. NaY, AgY, BaY, etc.) was used [31–35]. In addition, more than 50% NO_x conversions in a wide temperature range of 150–550 °C were obtained by combining BaY with Ag/Al_2O_3 in C_3H_6-SCR [36]. However, the role of NTP is still unclear for the complexity of reactions involved. The importance of NO oxidation [27,28] or the formation of hydrocarbon oxygenates [31,32,35,36] was supported by different researchers, respectively.

Study on the mechanism of HC-SCR with the assistance of NTP not only helps the application of NTP on NO_x removal, but also provides better understanding of thermal HC-SCR reactions especially at low temperatures, because the activation of reaction gas by NTP can provide abundant various species over Ag/Al_2O_3, which can not be obtained by thermal catalysis under such conditions. In this work, the formation and dynamic performance of the NTP-activated products from NO and C_3H_6 over Ag/Al_2O_3 were studied by an in situ DRIFTS method. Nitration and reduction are proposed as two main processes in HC-SCR. The activation of C_3H_6 in NTP can promote the nitration process by providing oxygenates or N-containing organics. Based on the evidences obtained, the role of ad-NO_x over Ag/Al_2O_3 is considered to be providing NO_2^+ species, which are essential both in the nitration process and in the reduction process.

2. Experimental

2.1. Catalyst preparation and characterization

Ag/γ-Al_2O_3 was prepared by a single-step sol–gel method. Aluminum (III) tri-isopropoxide (AIP) was first hydrolyzed at 85 °C on the evaporator with an appropriate amount of nitric acid solution (0.2 mol HNO_3/1 mol AIP) to form the sol. $AgNO_3$ solution in ethylene glycol was then slowly added into the sol solution by mixing for 1 h. The solvents were eliminated by heating under reduced pressure. The residue was then aged and gelled at room temperature. The obtained gel was dried at 110 °C for 24 h and calcined in air at 600 °C for 6 h. The final Ag/Al_2O_3 catalyst was 5 wt% and sieved to 0.15–0.28 mm for later use. γ-Al_2O_3 was prepared in the same way.

Surface areas and pore volumes of the alumina and the Ag/Al_2O_3 catalysts were determined on a QUANTASORB analyzer (Quantachrome Corporation). The samples were kept at 400 °C under vacuum (0.13 Pa) for 4 h before starting N_2 adsorption at liquid nitrogen temperature (77 K). Textual data are shown in Table 1. With loading of Ag, the BET surface area decreased slightly.

Table 1
The physical characteristics of the used catalysts

Support/catalyst	Specific area ($m^2\,g^{-1}$)	Pore volume ($cm^{-3}\,g^{-1}$)	Average pore diameter (nm)
Al_2O_3	233	0.29	7.5
5% Ag/Al_2O_3	202	0.22	6.9

2.2. Activity test

The system for activity test is of the PPCR (Post plasma catalytic reactor) type, in which non-thermal plasma was generated in a plate dielectric barrier discharge (DBD) reactor. Sinusoidal high voltage of 50 HZ varying between 6 and 10 kV was applied to excite the discharge. The catalysts were placed in a quartz tube reactor with an internal diameter of 6 mm downstream the plasma reactor. The catalytic reactor was held in a furnace where the temperature can be programmed. In most cases, the total flow rate of the feed gas was 100 mL/min and the dosage of catalyst was 0.25 g per test. The concentration of NO_x was analyzed by a NO-NO_2-NO_x analyzer (Thermo Electron Model 44). Propene and by-products after the reaction were examined online through a gas-phase chromatograph (Shimadzu GC 17A) or mass spectrograph (omni star).

2.3. Diffuse reflectance FT-IR analysis

The diffuse reflectance FT-IR measurements were carried out in situ in a high-temperature cell fitted with ZnSe windows. The samples were finely ground, directly placed in a ceramic crucible and manually pressed. The feed gas streamed into the cell at a total flow rate of 100 mL/min with or without non-thermal plasma pretreatment. The temperature in the cell can be programmed from 20 to 800 °C. Prior to analysis, all the samples were pretreated at 600 °C in a mixture of N_2 and O_2 for 60 min, then in N_2 for 30 min to remove the surface residents. The background spectra were collected after dwelling for 30 min at a given temperature. If not specified, the sample spectra reported here were collected after dwelling for 30 min. The spectra were recorded at a resolution of 4 cm^{-1}.

3. Results

3.1. Effect of NTP activation

In a typical PPCR (Post plasma catalytic reactor) system, when the feed gas is activated in NTP, all the gas components are activated by the impact of high-energy electrons and various kinds of products were generated which may have quite different behaviors in the later SCR reactions. The activation processes in NTP include the oxidation of NO, partial oxidation, N addition and nitration of hydrocarbon reductants, etc. In order to investigate which process is significant for SCR of NO, the effects of activating various gas components in NTP were examined in this section, respectively. The flow scheme of the experimental system is shown in Scheme 1. The gas components through the NTP reactor can be controlled by changing the valves.

3.1.1. Oxidation of NO

Fig. 1 shows NO_x and propene conversions when NO + O_2 (M1), O_2 (M2) and none (M3) in the feed gas were activated by NTP. In thermal SCR (M3), when the reaction temperature was below 350 °C, the propene conversion was very low (<11%) which corresponds to a low NO_x conversion of about 15% and indicates the difficulty of thermal catalytic activation of propene. When NO + O_2 in the feed gas was activated, NO_x and propene conversions were not obviously promoted in the temperature range of 250–300 °C. However the NO_x and propene conversions were increased by 17 and 24%, respectively, at 350 °C. O_3, which was often generated as one of the main byproducts of NTP in an

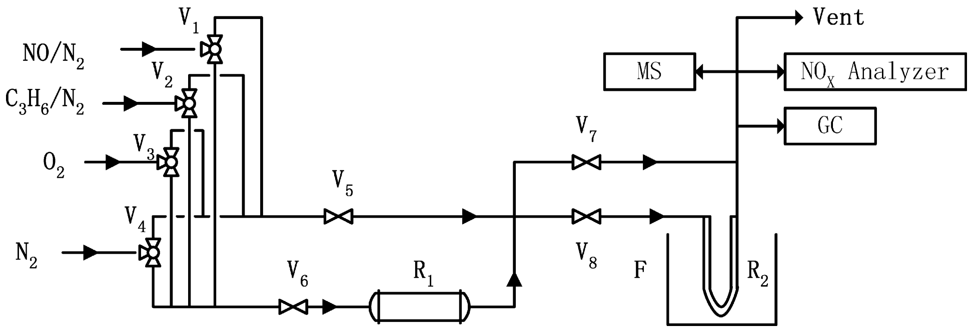

Scheme 1. Flow scheme of the experimental system for activity evaluation. F, Furnace; R_1, non-thermal plasma reactor; R_2, catalytic reactor; V_1–V_4, three-way valve; V_5–V_8, open-closed valve; GC, gas chromatograph; MS, mass spectrograph.

oxygen-rich atmosphere, contributed to the oxidation of NO. The results of M2 showed the effect of O_3 on SCR activities. It is interesting that a negative peak of NO_x conversion was observed at 300 °C. This might be resulted from the decomposition of O_3, leading to the formation of quenched intermediates and a relatively low activity of SCR. As temperatures were higher than 300 °C, the catalytic oxidation of propene became active and then the activity of SCR increased.

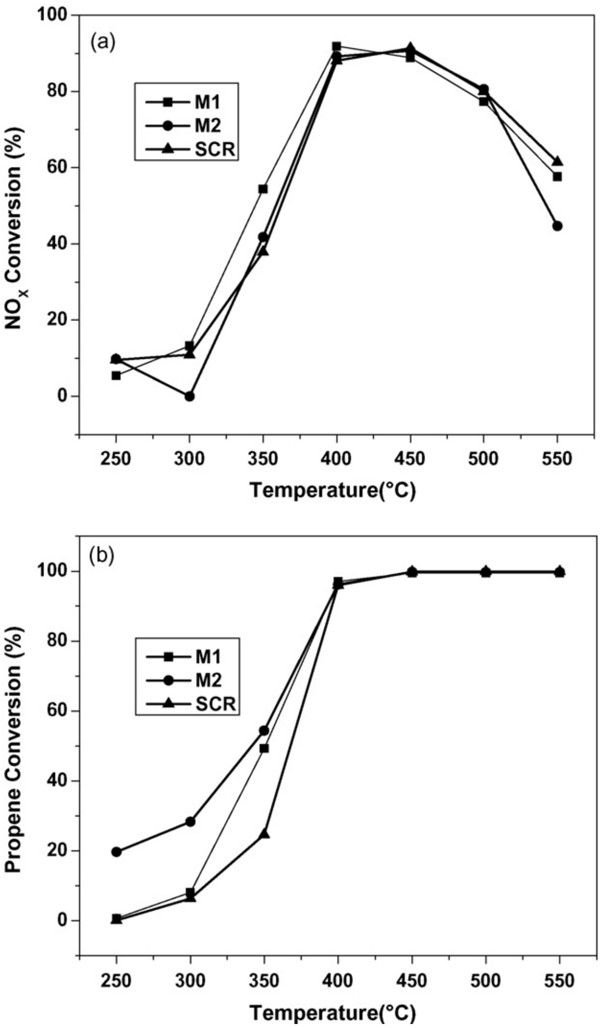

Fig. 1. Conversions of NO_x (a) and propene (b) when NTP was used to activate $NO + O_2$ (M1), O_2 (M2) and none (SCR) in the reaction gas. Conditions: C_3H_6, 1000 ppm; NO, 1000 ppm; O_2, 8%; balance gas, N_2; flow rate 100 mL/min.

3.1.2. Activation of propene

Fig. 2 shows the influence of propene activation by NTP in different atmosphere of $C_3H_6 + N_2$ (C1), $C_3H_6 + N_2 + O_2$ (C2), $C_3H_6 + N_2 + O_2 + NO$ (C3) and C_3H_6 (C4). When the reaction temperature was below 350 °C, it was found that the propene activation in all the cases above enhanced the NO_x conversion of SCR. The activation atmosphere in NTP was quite essential to the reaction activity in the temperature range of 250–550 °C. As shown in C4, the promoting effect of activating propene in helium was the lowest in all cases below 350 °C. Meanwhile, the NO_x conversion was much lower (<58%) than that of thermal SCR above 350 °C.

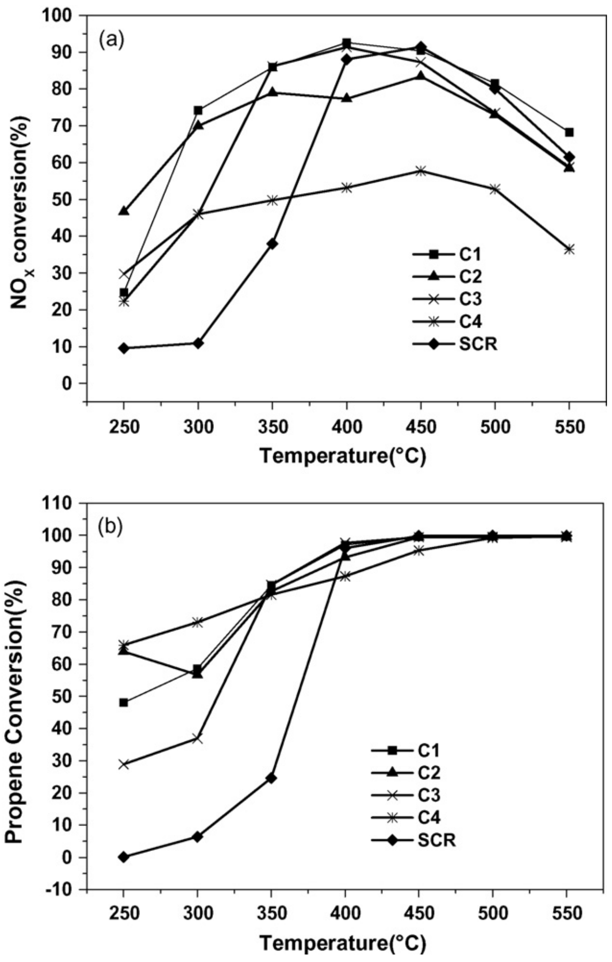

Fig. 2. Conversions of NO_x (a) and propene (b) when NTP was used to activate $C_3H_6 + N_2$ (C1), $C_3H_6 + N_2 + O_2$ (C2), $C_3H_6 + N_2 + O_2 + NO$ (C3), C_3H_6 (C4) and none (SCR) in the reaction gas. Conditions: C_3H_6, 1000 ppm; NO, 1000 ppm; O_2, 8%; balance gas, N_2; flow rate 100 mL/min.

When O_2 was in the presence of propene activation (C2), the corresponding NO_x conversion was obviously promoted below 300 °C, although it decreased slightly above 450 °C as compared with that of thermal SCR. Interestingly, propene activation in N_2 (C1) demonstrated high NO_x conversions at the reaction temperatures between 250 and 550 °C although its NO_x conversion was lower than those of C_2 and C_3 at 250 °C. When propene was activated by NTP in an atmosphere of O_2, N_2 and NO (C3), the NO_x conversion was just between those of C1 and C2.

It is found in Fig. 2b that, after being activated in various environments in NTP, the conversions of propene below 350 °C was obviously enhanced as compared with thermal SCR. The propene conversion of C3 was relatively lower than those of other cases although its NO_x conversion was not the lowest, which suggests that the activating environments in NTP would influence the utilization of propene.

3.1.3. Direct decomposition of NO

Fig. 3 shows the NO_x and propene conversions when NTP was used to activate NO in the reaction gas. At the low temperatures of 200 °C the NO_x conversion has already reached 95%. When SCR reactions were active above 300 °C, more of 4% NO_x conversion was achieved. Apparently, the high NO_x conversion was mainly contributed by direct decomposition of NO in NTP, during which NO was dissociated by high-energy electrons in NTP to generate the activated atomic N^* radicals and the N^* radicals reacted with NO to generate N_2 [37–39]:

$$N^* + NO \rightarrow N_2 + O \tag{1}$$

In thermal and NTP-assisted SCR, propene conversion was completely consumed at about 400 °C while in this case the temperature of complete propene conversion shifted to 500 °C. Since most NO was decomposed in NTP, little NO was remained in the reactions over Ag/γ-Al_2O_3. This phenomenon suggests that NO_x can promote the propene conversion in SCR.

3.2. Influence of NTP activation on NO adsorption

Since NO can hardly initiate a direct reaction with propene, one important step in HC-SCR is the adsorption of NO during which NO is oxidized and converted to absorbed NO_x (ad-NO_x). Fig. 4 shows the DRIFTS spectra of species in NO + O_2 adsorption over Ag/Al_2O_3 at 50 and 400 °C, respectively. In order to clarify the influence of NTP activation of NO + O_2 on the formation of ad-NO_x, corresponding spectra were also present. After NO + O_2 was absorbed over Ag/Al_2O_3 for 30 min at 50 °C, typical bands for nitrates and nitrite were observed. They were unidentate nitrate at 1556 and 1245 cm^{-1}, bidentate nitrate at 1585 and 1296 cm^{-1}, bridging nitrate at 1620 cm^{-1} [23,24,26]. When NO + O_2 was activated in NTP before absorbed over Ag/Al_2O_3, bands for the ad-NO_x species above were also observed. However, the distribution of these bands was quite different from that in natural NO + O_2 adsorption. Bands and shoulders in 1500–1700 cm^{-1} were apparently weaker than those in 1200–1400 cm^{-1}. Moreover, strong new bands at 1416 and 1470 cm^{-1} were additionally observed. Since NO was partially oxidized to NO_2 and O_2 was converted to O_3 in NTP, this difference between NTP-NO + O_2 and NO + O_2 adsorption must be resulted from the influence of O_3 on ad-NO_x species. The new bands may be attributed to the species generated in the reaction between ad-NO_x and O_3.

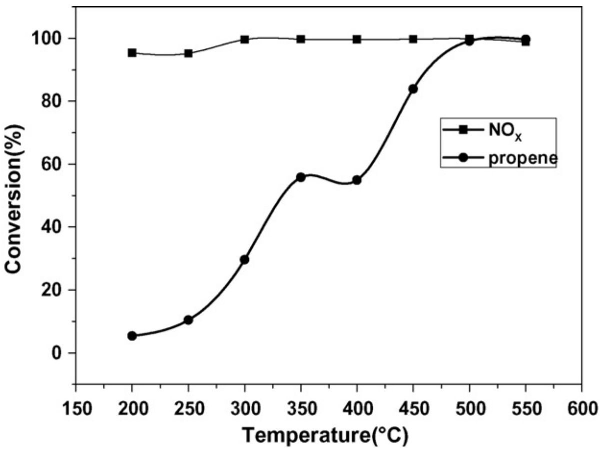

Fig. 3. Conversions of NO_x and propene when NTP was used to activate NO in the reaction gas. Conditions: C_3H_6, 1000 ppm; NO, 1000 ppm; O_2, 8%; balance gas, N_2; flow rate 100 mL/min.

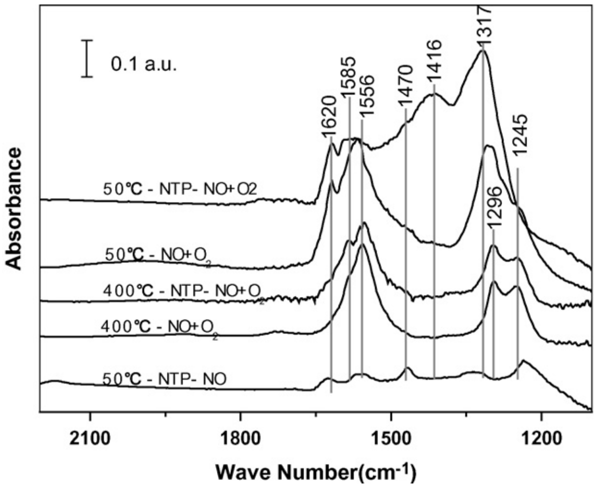

Fig. 4. DRIFTS spectra of ad-NO_x species in the adsorption of NO + O_2 over Ag/Al_2O_3 with or without the assistance of NTP. Conditions: NO, 1000 ppm; O_2, 8%; balance gas, N_2.

At higher temperature of 400 °C, the spectra of NTP-NO + O_2 and NO + O_2 adsorption were quite similar. The bands in 1500–1400 cm^{-1} were disappeared, which must be resulted from both the desorption of ad-NO_x and the rapid decomposition of O_3. The bands in the spectra for NTP-NO adsorption over Ag/Al_2O_3 at 50 °C are all very weak. It is reasonable since most NO is decomposed in NTP as seen in Section 3.1.3.

3.3. Thermal oxidation and consumption of C_3H_6 in SCR

Fig. 5 shows the DRIFTS of C_3H_6 + O_2 adsorption over Ag/γ-Al_2O_3. Many species have peaks in the region of 3200–2500 cm^{-1}, including –CH_3 (2945, 2983 cm^{-1}), –CH_2– (2925, 2859 cm^{-1}), –CH (2910 cm^{-1}) and $HCOO^-$ (3000 cm^{-1}) [23,24,26,40]. At 50 °C, the weak bands observed in the region of 3200–2500 cm^{-1} should be mainly due to the adsorption of C_3H_6. As the temperature increased, the intensities of these bands weakened and almost disappeared at 200 °C, which should be attributed to desorption of C_3H_6. When the temperature was raised again, new bands at 3200–2500 cm^{-1} appeared and strengthened. This should be attributed to the formation of formate and acetate species. At 500 °C the weak band assignable to symmetric stretching of –CH (2910 cm^{-1}) disappeared, which indicated the decrease of $HCOO^-$ species.

Strong absorbance bands, observed at 1572 and 1458 cm^{-1} above 300 °C, have mainly been attributed to surface acetate in most reports [23–26,40–42]. The intensities of these bands increased with temperature and were still very strong at 500 °C.

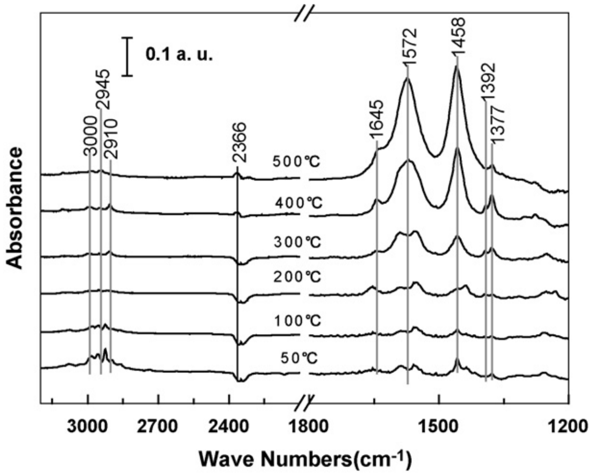

Fig. 5. DRIFTS spectra of species during the adsorption of $C_3H_6 + O_2$ over Ag/γ-Al_2O_3 under various temperatures. Conditions: C_3H_6, 1000 ppm; O_2, 8%; balance gas, N_2.

This suggests that the surface acetate species are stable at high temperatures. The weak bands attributable to formate were also observed at 1392 (δ_{CH}) and 1377 cm^{-1}, whose variations with temperature were similar to the band at 2910 cm^{-1}. The band at 1645 cm^{-1} was once assigned to the vibration of C=O [40] or organo-nitro species [26]. It should be more appropriate to assign this band to enolic species, based on the study of C_2H_5OH-SCR over Ag/Al_2O_3 [22,24,42,43]. Weak bands for CO_2 were found at 2366 cm^{-1} [40–43] above 400 °C, indicating that the total oxidation of surface organic species occurred at this time.

Fig. 6 shows the dynamic change of species during C_3H_6-SCR under various reaction temperatures. Since the partial oxidation of propene took place obviously above 200 °C, the experimental temperature was selected above 200 °C in this case. Although the presence of NO caused the formation of weak peaks of –NCO (2240 cm^{-1}) and –CN (2156 cm^{-1}) [25] over Ag/γ-Al_2O_3, the oxidation process of propene showed no obvious change. CO_2 (2366 cm^{-1}) occurrence and formate (2910, 1392, 1377 cm^{-1}) disappearance were at the same temperature (shown in Fig. 5). The change of acetate (1572, 1458 cm^{-1}) and enolic species (1645 cm^{-1}) with temperature was also similar. This suggested that NO in the feed gas did not change the light off temperature of the partial oxidation of C_3H_6. Though acetate species were found to be abundant above 450 °C, the NO_x conversions were decreased with temperature in this temperature region.

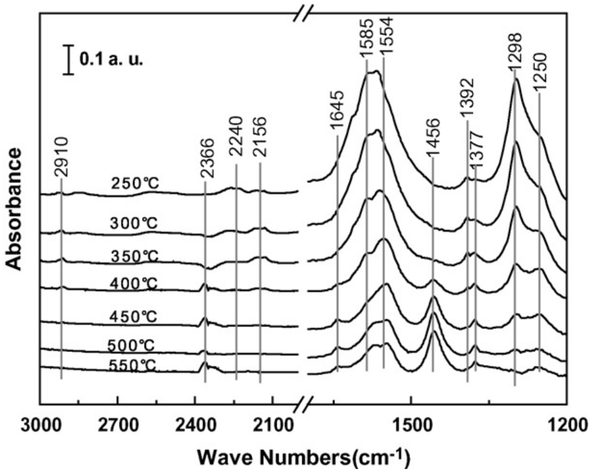

Fig. 6. DRIFTS spectra of C_3H_6-SCR over Ag/γ-Al_2O_3 under various reaction temperatures. Conditions: C_3H_6, 1000 ppm; NO, 1000 ppm; O_2, 8%; balance gas, N_2.

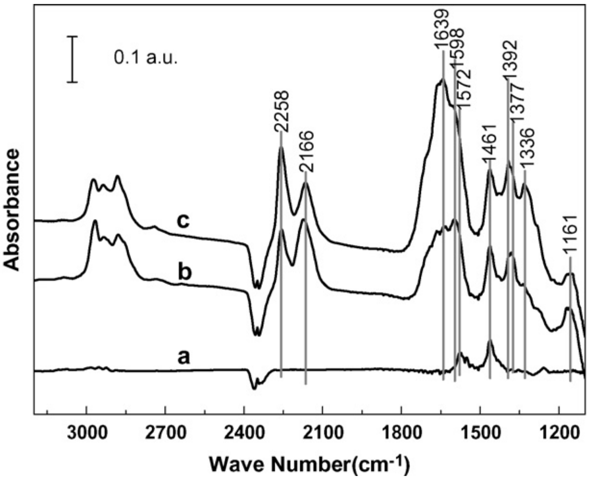

Fig. 7. DRIFTS spetra of species over Ag/Al_2O_3 at 100 °C during the adsorption of the products from activating C_3H_6 in an N-predominant environment in NTP: streaming C_3H_6 and dwelling for 30 min (a), activating C_3H_6 in N_2 by NTP and dwelling for 30 min (b), activating C_3H_6 in N_2 + NO by NTP and dwelling for 30 min (c). Conditions: C_3H_6, 1000 ppm; NO, 1000 ppm.

3.4. Activation and consumption of C_3H_6 in NTP-SCR

The activation of C_3H_6 in various atmospheres in NTP leads to different activation products and causes the variety of influence on the SCR reactions over Ag/Al_2O_3. Fig. 7 shows the absorbed species of the products from C_3H_6 activation in various atmospheres in NTP over Ag/γ-Al_2O_3 at 100 °C. Species of C_3H_6 adsorption are present in spectrum (a) of Fig. 7 as a comparison. The bands attributable to C_3H_6 were very weak in spectrum (a). As C_3H_6 was activated only in the carrier gas N_2, strong bands attributable to –NCO (2258 cm^{-1}) and –CN (2166 cm^{-1}) were observed in spectrum (b). Apparently, the N atom in –NCO and –CN must come from balance gas N_2 since no other N-containing reactants were in the feed gas. In NTP, N_2 and propene was decomposed by high energy electrons into atomic N^*, methyl and other radicals. In the reactions between these radicals and propene, various kinds of N-containing species (i.e. R-CN) were formed. The surface species, –NCO, should be generated from the bonding of R-CN with the oxygen form the catalyst, because no O_2 was in the stream. Strong peaks for enolic species (1639, 1416, 1336 cm^{-1}), acetate (1572, 1461 cm^{-1}) and formate (1392, 1377 cm^{-1}) were also observed, indicating that the activated products of propene can easily be oxidized to oxygenates by the oxygen from Ag/Al_2O_3. When NO was added into the stream (spectrum c), the intensity of isocyanate species and oxygenates increased remarkably, whereas that of –CN remained nearly unchanged. This is probably due to the addition of NO to C=C bond in propene to form $C_xH_yO_zN$ species which show the –NCO bands after absorbed over Ag/γ-Al_2O_3 at 100 °C. Another possibility is the introduction of oxygen through NO favored the oxidation of $C_xH_yN_z$ compounds in NTP, because NO can easily be dissociated to N_2 and O_2 in NTP.

Fig. 8 shows the effect of O_2 on propene activation in NTP and the variation of species when the activated products were absorbed over Ag/Al_2O_3 at 50 °C. In Fig. 8A, it is seen that abundant –NCO and –CN species were formed when propene was activated in N_2 in NTP (spectrum 1). Interestingly, although the addition of O_2 effectively increased the quantities of important SCR species such as enolic (1639, 1336 cm^{-1}) and acetate (1464 cm^{-1}), the quantities of –NCO and –CN simultaneously were decreased

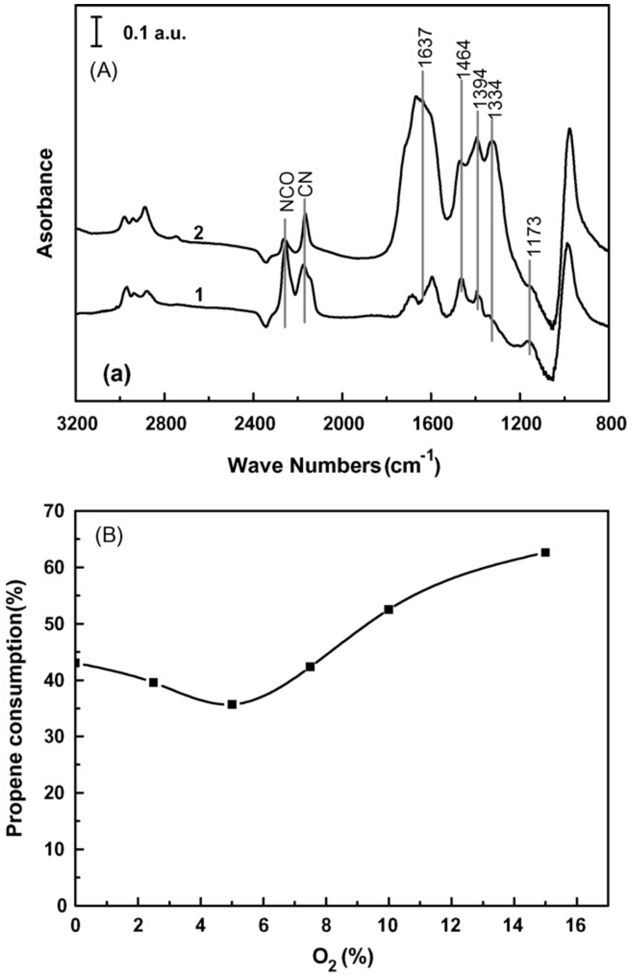

Fig. 8. (A) Comparison of species over Ag/Al_2O_3 at 50 °C, during the adsorption of the products for activating C_3H_6 in N_2 (1) and $N_2 + O_2$ (2) in NTP. (B) The effect of O_2 on the activation of C_3H_6 in NTP. Conditions: C_3H_6, 1000 ppm; O_2, 8%.

(spectrum 2). This may be attributed to two reasons: firstly, (1) –NCO and –CN species are chemically unstable under an oxidizing environment; secondly, the formation of $C_xH_yN_z$ products in NTP was suppressed. Fig. 8B shows the relationship between C_3H_6 consumption and O_2 concentration in NTP at room temperature. Under the condition of little O_2, the conversion of propene is mainly contributed by the reactions with N^* radicals. As the concentration of O_2 increases, the formation of N^* radicals is suppressed which decreases the propene consumption. If the concentration of O_2 continues to increase, the oxidation of propene by O_2 become predominant which promotes the C_3H_6 consumption again. High concentration of O_2 results in the increase of O-containing organic products and the decrease of N-containing organic products, simultaneously.

Spectra in Fig. 9 proved that the products of $C_3H_6 + NO + N_2$ generated in NTP have evident reactivity to $NO + O_2$ over Ag/Al_2O_3. After switching to $NO + O_2$, the bands corresponding to –NCO (2231 cm^{-1}), –CN (2131 cm^{-1}), enolic species (1639, 1336 cm^{-1}), acetate (1570, 1460 cm^{-1}) and formate (1394, 1377 cm^{-1}) were weakened. In the first 15 min, the intensity of bands for –NCO, –CN, formate and enolic species decreased much faster than those for acetate, suggesting that these species had higher reactivity than acetate. Interestingly, –CN group was disappeared at 15 min (spectrum 2) and occurred again after 60 min (spectrums 3–5). The former –CN should be generated by N-containing hydrocarbon species in the reductant stream and the later –CN may be from the reactions of oxygenates with $NO + O_2$.

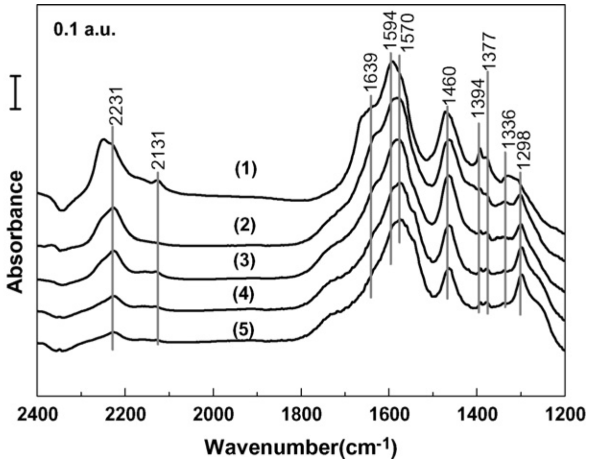

Fig. 9. Dynamic change of species over Ag/Al_2O_3 at 350 °C in the following operations: (1) adsorption of the products from activating $NO + C_3H_6$ in NTP for 30 min, (2) switching the reaction gas to $NO + O_2$ and passing it directly to the catalyst for 15 min, (3) 60 min, (4) 150 min and (5) 210 min. Conditions: NO, 1000 ppm; C_3H_6, 1000 ppm; O_2, 8%, balance gas, N_2.

Fig. 10 shows the dynamic change of species during NTP-assisted SCR under various reaction temperatures. It is seen that, under fairly low temperatures (i.e. 50 °C), isocyanate groups were generated over $Ag/\gamma\text{-}Al_2O_3$. Strong bands for acetate, formate and enolic species were simultaneously observed which were much stronger than those found in SCR reactions under the similar condition (see Fig. 6). In the temperature range of 50–250 °C, the peak intensity of bands for enolic species decreased (1645 cm^{-1}) meanwhile that of isocyanate species (2258 cm^{-1}) increased, indicating that enolic species are reactive to generate isocyanate species. At a low temperature of 250 °C, evident bands were observed for CO_2 which was an indirect evidence for NO_x reduction [42]. Although isocyanate, enolic species and nitrates were apparently abundant below 250 °C, no obvious activities for NO_x reduction were observed. The NO_x conversions above 450 °C were lower in NTP-assisted SCR than in thermal SCR despite the fact that the concentration of isocyanate species were apparently higher in the former one. The reasons will be discussed below.

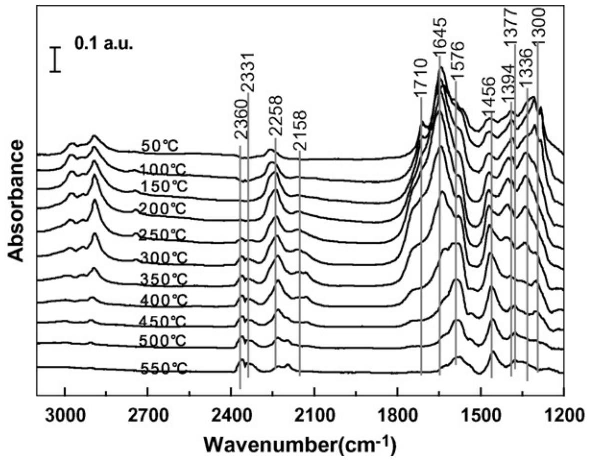

Fig. 10. Dynamic change of species in NTP-assisted SCR over Ag/Al_2O_3 under various reaction temperatures. Conditions: C_3H_6, 1000 ppm; NO, 1000 ppm; O_2, 8%; balance gas, N_2.

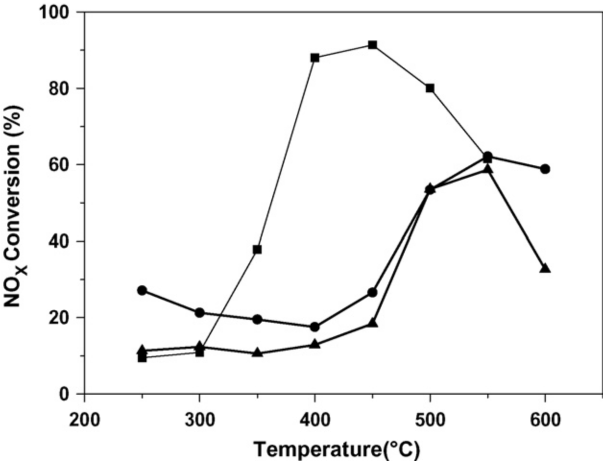

Fig. 11. NO$_x$ conversions under the following process: SCR over fresh Ag/Al$_2$O$_3$ (■), SCR over sulfated Ag/Al$_2$O$_3$ exposing to SO$_2$ (▲), NTP-SCR over sulfated Ag/Al$_2$O$_3$ exposing to SO$_2$ (●). Conditions: NO, 1000 ppm; C$_3$H$_6$, 1000 ppm; O$_2$, 8%; SO$_2$, 100 ppm; balance gas, N$_2$. The sulfated Ag/Al$_2$O$_3$ was obtained by treating the fresh Ag/Al$_2$O$_3$ sample in the stream of 100 ppm SO$_2$ + 8% O$_2$ for 24 h.

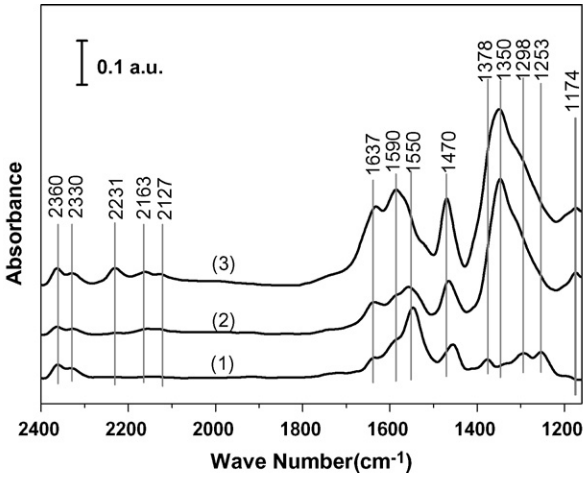

Fig. 13. Dynamic changes of DRIFTS spectra over Ag/Al$_2$O$_3$ at 450 °C during the process of SCR for 40 min (1), adding SO$_2$ into the feed gas and dwelling for 40 min (2), turning on non-thermal plasma for NTP-SCR for 40 min (3). Conditions: NO, 1000 ppm; C$_3$H$_6$, 1000 ppm; O$_2$, 8%; SO$_2$, 100 ppm; balance gas, N$_2$.

3.5. Sulfidation effect in SCR and NTP-SCR

Fig. 11 shows the SO$_2$ effects on both thermal SCR and NTP-assisted SCR over Ag/Al$_2$O$_3$. In thermal SCR without SO$_2$ poisoning, the effective temperature window covered from 400 to 550 °C over fresh Ag/Al$_2$O$_3$ with NO$_x$ conversion above 60%. After the Ag/Al$_2$O$_3$ sample was poisoned by SO$_2$ for 24 h, the activities in the temperature range of 300–550 °C were obviously decreased both in thermal SCR and in NTP-assisted SCR with 100 ppm SO$_2$ in the feed gas. The assistance of NTP provided an activity enhancement of only 7–20% below 400 °C in presence of SO$_2$ over the sulfated Ag/Al$_2$O$_3$, which was far lower than that could be achieved over fresh Ag/Al$_2$O$_3$ sample in absence of SO$_2$.

Fig. 12 shows the dynamic changes of species over Ag/Al$_2$O$_3$ in the NO + O$_2$ adsorption process that was influenced by SO$_2$ and C$_3$H$_6$. After NO + O$_2$ adsorption for 40 min, strong peaks at 1583, 1552, 1297 and 1250 cm^{-1} were observed over the fresh Ag/Al$_2$O$_3$ sample, which could be, respectively, assigned to various kinds of nitrates. After 100 ppm SO$_2$ was added into the feed gas and dwelled for 100 min, obvious decrease of peaks at 1583 and 1552 cm^{-1} occurred. This indicated that these two kinds of existed nitrate species were decomposed or converted to other species by competition adsorption of SO$_2$. Meanwhile, strong peaks attributable to silver sulfate (1360, 1276 cm^{-1}) and aluminum sulfate (1170, 1317 cm^{-1}) were observed to increase with time [43]. At this time, stopping SO$_2$ in the feed gas and dwelling for 120 min did not cause the recovery of nitrate species and lose of ad-SO$_2$ species. This suggested that the surface sulfate species were more stable than nitrates and occupied the basic adsorption sites over Ag/Al$_2$O$_3$ to baffle the adsorption of NO. After consecutively adding 1000 ppm C$_3$H$_6$ into the feed gas and dwelling for 30 min, enolic (1635 cm^{-1}) and acetate species (1464 cm^{-1}) occurred while the sulfate species did not change.

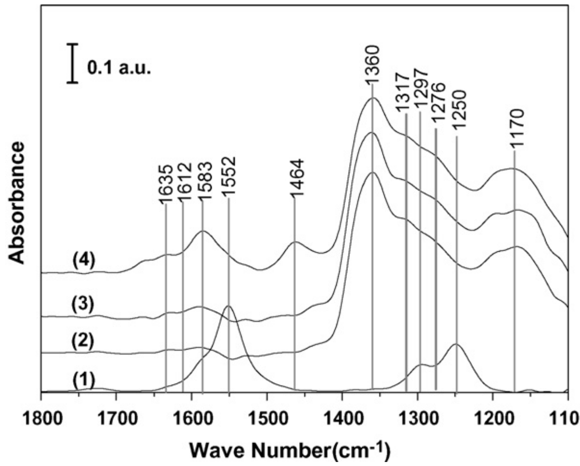

Fig. 12. Dynamic changes of DRIFTS spectra over Ag/Al$_2$O$_3$ at 400 °C in the following steps: NO + O$_2$ adsorption for 40 min (1), adding SO$_2$ into the feed gas and dwelling for 100 min (2), stopping SO$_2$ and dwelling for 120 min (3), adding C$_3$H$_6$ into the feed gas and dwelling for 30 min (4). Conditions: NO, 1000 ppm; C$_3$H$_6$, 1000 ppm, SO$_2$, 100 ppm; O$_2$, 8%, balance gas, N$_2$.

Fig. 13 shows the species in SCR and NTP-SCR in presence of SO$_2$ over Ag/Al$_2$O$_3$. After SO$_2$ was added, obvious sulfate species occurred at 1350 and 1174 cm^{-1} with the decrease of nitrate species at 1550 cm^{-1}. With the assistance of NTP, the amount of isocyanate species (2231 cm^{-1}) and enolic species (1637 cm^{-1}) increased. However, no promoting effect was observed for the nitrate species at 1550 cm^{-1}. Relating to the low NO$_x$ conversions of NTP-assisted C$_3$H$_6$-SCR in presence of SO$_2$, it is obvious that the assistance of NTP did not enhance the SO$_2$ resistance. Since isocyanate species, enolic species and gas phase NO$_x$ were abundant, the low activities of NTP-assisted SCR in presence of SO$_2$ must be attributed to the lack of surface nitrates under such conditions. In addition, this suggested that the reaction between isocyanate and gas phase NO$_x$ was not possible or not essential for NO$_x$ reduction, which was once regarded as one of the important pathways for N$_2$ generation.

4. Discussion

4.1. Role of the products from the activation of reaction gas in NTP

Most components in the reaction gas can be partly dissociated or ionized by the impact of high-energy electrons in NTP. During this process, propene can be dissociated into methyl, atomic H and other organic radicals. NO, N$_2$ and O$_2$ can also be dissociated into atomic N and O radicals. These radicals are highly reactive and rapidly react with each other or the original gas molecules to form various kinds of products including aldehydes, organic acids or N-

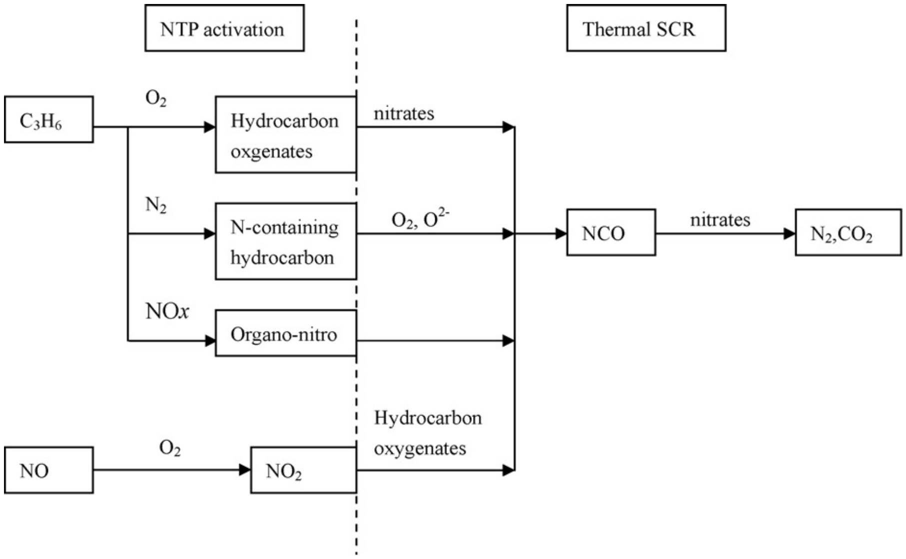

Fig. 14. Roles of the products from the activation of reaction gas in NTP.

containing organics, etc., which influence the latter SCR reactions over the Ag/γ-Al_2O_3 catalyst (Fig. 14).

When NO and O_2 was present in NTP, NO was effectively oxidized to NO_2 by O_3 and atomic oxygen radicals, which was easier than NO to form the surface nitrates over the catalyst and react with propene. The oxidation of NO was once considered to be the reason why NTP enhanced the low temperature activities of HC-SCR. However, as shown in Fig. 4, NO can easily converted to various kinds of surface nitrates and nitrites over Ag/γ-Al_2O_3 even at very low temperatures. The results in Section 3.1.1 show that the oxidation of NO and O_3 formation in NTP were not important for SCR reactions over Ag/γ-Al_2O_3 below 350 °C. We have investigated the influence of replacing NO with NO_2 in the reaction gas and found no obvious promotion in NO_x conversion. Although the activation of NO was not important in NTP-assisted C_3H_6-SCR, it was believed to have changed the proportion of various ad-NO_x species over Ag/γ-Al_2O_3.

As for Ag/γ-Al_2O_3, the main barrier to obtain high NO_x conversions below 350 °C was the difficulty of activating propene. DRIFTS spectra in Figs. 5 and 6 suggested that propene could only be effectively activated above 300 °C by the thermal catalysis over Ag/γ-Al_2O_3 and the addition of NO did not change the activation energy of this process. NTP offers another way to activate propene at various temperatures. The conversion of propene increased quickly after NTP was applied and the NO_x conversions below 350 °C were remarkably enhanced (Fig. 2). Activity enhancements were also achieved with the activating propene in various environments in NTP, due to the influence of different kinds of products as discussed below.

Hydrocarbon oxygenates are the main products when propene is activated in an O-predominant environment (i.e. in presence of enough O_2) in NTP, which are formed by reactions among O radicals, O_3, propene and methyl radicals, etc. DRIFTS of NTP-assisted SCR proved that abundant hydrocarbon oxygenates species mainly including formate, acetate and enolic species were formed over Ag/γ-Al_2O_3 downstream the NTP reactor even at low temperatures. These hydrocarbon oxygenates are believed to be important precursors of the key intermediate R-NO_2 and –NCO in NO_x reduction and favored the NO_x reduction at low temperatures. As compared with thermal C_3H_6-SCR, the NO_x conversions between 250 and 350 °C were obviously enhanced under these conditions. However, strong oxidation of propene seemed not favorable for NO_x reduction at high reaction temperatures. The generated oxygenates were easily oxidized to CO_2 which led to a decrease of NO_x conversion due to the lack of reductants. In addition, part of propene might be oxidized to CO_2 directly in NTP.

N-containing organics ($C_xH_yO_zN$ or C_xH_yN) are another kind of products in NTP, when propene is activated in an N-predominant environment (i.e. only in N_2), which are formed by reactions among N radicals, propene and methyl radicals. These $C_xH_yO_zN$ species were another origin of –NCO over Ag/γ-Al_2O_3 besides the reaction between nitrates and oxygenate species. The C_xH_yN species can easily generate CN species (through adsorption) or –NCO species (through directly oxidation by the oxygen from the catalyst) over Ag/Al_2O_3 (Fig. 7). In addition, the $C_xH_yO_zN$ products (i.e. RNO_2 or RONO, etc.) can also generate –NCO species through direct decomposition over Ag/Al_2O_3 [26]. The generated –NCO and –CN species were reactive to NO_x or surface nitrates at 350 °C as shown in Fig. 9. The corresponding NO_x and propene conversions were also found much higher than the thermal C_3H_6-SCR between 300 and 400 °C. It is interesting that the NO_x conversions above 400 °C were not deteriorated due to the activation of propene by NTP under this condition, as compared with the results when propene was activated in an O-predominant environment in NTP. In an atmosphere that both O_2 and N_2 existed, the generation of N-containing organics products was strongly suppressed when the concentration of O_2 exceeded 5% (Fig. 8), due to the easier dissociation of O_2 than N_2 in NTP. However, even in an O-predominant in presence of NO, theoretical [44] and experimental [35] studies revealed that part of the hydrocarbon could be converted to organo-nitro or RCN species directly in NTP.

4.2. Nitration and reduction in HC-SCR

Although there are many important steps in HC-SCR reactions, including the oxidation and adsorption of NO, partial oxidation of reductants and the reduction of ad-NO_x, etc., they can be classified into two kinds of reaction, namely *nitration* and *reduction*. The so-called *nitration* means the reactions to provide organo-nitro species, and the *reduction* means the reactions to generate N_2 involving isocyanate species and ad-NO_x species over Ag/Al_2O_3.

4.2.1. The nitration process in HC-SCR

In fine chemistry, nitration is a kind of typical and important reactions to produce the N-containing chemicals and has been adequately studied for decades. Although not easily observed by spectroscopy, NO_2^+ is regarded as the key intermediates of nitration, which starts from the attack of NO_2^+ to electron-rich organic groups [45].

Organic compounds which are rich of electrons or can be easily dissociated into electron-rich function groups over catalysts are favorable to react with NO_2^+. This is also applicable in the nitration process in HC-SCR. Many studies on the HC-SCR reactions over metal oxide catalysts have revealed that if a reaction system is easier to provide electron-rich species (i.e. enolic species, COO^-, etc.), it can achieve higher NO_x conversions. A typical example is the difference between ethanol-SCR and C_3H_6-SCR over Ag/Al_2O_3. Yu et al. [24] concluded that the higher activities of NO_x reduction in ethanol-SCR than in C_3H_6-SCR below 400 °C were the abundance of enolic species ($CH_2{=}CH{-}O^-$) from the activation of ethanol over Ag/Al_2O_3. The influence of activating propene in an O-predominant atmosphere in NTP was similar to providing oxygenate reductants for SCR reactions over Ag/Al_2O_3. Considerable amount of propene was converted to acetaldehyde when the reaction gas of $C_3H_6 + O_2 + NO$ was activated in NTP [35], which was also active in NO_x reduction over Ag/Al_2O_3 [24]. When propene was activated in an N-predominant environment in NTP, the direct formation of isocyanate species during the adsorption of $C_xH_yO_zN$ over Ag/Al_2O_3 avoided the resistance in the thermal nitration process and could be considered as a promotion of nitration, leading to high activities of NO_x reduction above 300 °C.

Another kind of important species in the nitration process is nitroium (NO_2^+). Nitric acid and nitrates (i.e. $AgNO_3$) are typical carriers of NO_2^+, which generally release NO_2^+ over the catalysts. In HC-SCR over Ag/Al_2O_3, the ad-NO_x species from NO oxidation and adsorption should act as the role of NO_2^+ carriers. Organo-nitro or isocyanate species in HC-SCR were regarded to be from the reaction between enolic species (or acetate) and nitrates. However, the studies of ethanol-SCR showed that the concentration of isocyanate species and corresponding NO_x conversions were fairly low despite high concentrations of surface enolic species and nitrates below 250 °C [24,44]. Recently, the influence of ad-NO_x has been becoming an interest of research, especially on the activities of HC-SCR at low temperatures [46]. We speculate that the inability of ad-NO_x to provide enough NO_2^+ species is the main resistance under such conditions. The formation of NO_2^+ is probably an interim step in the decomposition of surface nitrates into NO_2. Studies on the adsorption of NO_x over Ag/Al_2O_3 catalysts showed that the ad-NO_x species bonded to Ag^+ were quite stable below 250 °C [46], leading to the difficulty to provide nitroium. Metallic silver was found to be much more effective than Ag^+ to catalyze the NO oxidation in O_2 for the instability of ad-NO_x over it [16,47]. Some researchers found an obvious promoting effect of H_2 in HC-SCR over Ag/Al_2O_3 below 250 °C and the role of H_2 as reductant was excluded [46,48,49].

The reduction of Ag^+ to metallic silver was proposed as the origin of this promotion effect. Although the partial oxidation of hydrocarbon by metallic silver (or OH radicals from H_2) might contribute to the HC-SCR, the activity of ad-NO_x to provide NO_2^+ over Ag^0 should also be important, especially in ethanol-SCR, in which the activation of the reductant is already active below 250 °C. Other evidences for the importance of NO_2^+ in the reduction process will be further discussed below, based on the study in this paper.

According to the studies on the protonation of nitrates and nitrites [50], H^+ from the catalysts generally enhances the stability of NO_2^+ and favors the nitration process. As compared with the metal oxide catalysts, zeolite catalysts (i.e. NaY, BaY, etc.) was found to be more effective in the NTP-assisted C_3H_6-SCR below 200 °C [31–34]. One reason for this difference could be attributed to the abundance of B acid sites over zeolite catalyst, which is favorable to the formation of NO_2^+ and promotes both the nitration and reduction process in SCR in presence of abundant oxygenate species provided by NTP assistance. The increase of acidity was also regarded as an importance contributor for the activity promotion over the modified (i.e. by appropriate amount of ZnO) alumina-supported, especially at low temperatures [51].

4.2.2. The reduction process in HC-SCR

The reduction steps were considered to be fast steps in HC-SCR reactions, among which

$$NCO + NO_3^- \,(\text{or}\, NO_x) \rightarrow N_2 + CO_2 \qquad (2)$$

the above reaction was often mentioned as the final step. The amount of isocyanate species, acting as the reductant, is determined by the nitration steps in HC-SCR. Gas phase NO_x was once considered to be able to react with isocyanate species directly, however, the study on the sulfidation effect of NTP-SCR (Fig. 13) showed that the isocyanate species could only react with surface nitrates, based on the facts that the absence of surface nitrates caused the low efficiency of NO_x reduction even in presence of enough isocyanate species at 400 °C. Similar to the nitration process, the role of nitrates in the reduction process was also suggested to provide NO_2^+, because no obvious NO_x conversions were observed in NTP-SCR below 200 °C (not shown here) despite the abundance of isocyanate and nitrates species as shown in IR spectra of Figs. 7, 8 and 10. The surface nitrates were quite stable below 200 °C over Ag/Al_2O_3. Although –NCO, –CN and enolic species can be generated with the assistance of NTP, the inability of the stable nitrates to provide NO_2^+ species baffles the reduction process of SCR.

The typical steps in the nitration and reduction process of thermal HC-SCR over Ag/Al_2O_3 are summarized in Fig. 15, among which two kinds of competitive reactions should be emphasized for their influences on the effectiveness of NO_x reduction. The first is the competition for nitrates (essentially NO_2^+) between the nitration and reduction process. As the nitration proceeds extremely fast and consumes too much surface nitrates, the lack of nitrates suppresses the reduction process and the excessive part of RNO_2, –NCO and –CN species will be oxidized back to NO_x by O_2. This effect was found in the C_3H_6-SCR over the SnO_2-doped Ga/Al_2O_3 catalyst that, although SnO_2 promoted the reaction between NO and C_3H_6, the efficiency of NO_x reduction was decreased for the excessively oxidation of N-containing intermediates [52]. The second is the competition of –NCO species between its reaction with nitrates to generate N_2 and its oxidation by O_2 to NO_x. At high reaction temperatures, the lack of nitrates and the oxidation of –NCO species may both exist in HC-SCR. In thermal C_3H_6-SCR over Ag/Al_2O_3 above 450 °C, the amount of reductant species (acetate and enolic species) did not obviously decreased whereas the NO_x conversion did, which can be related to the lack of surface nitrates

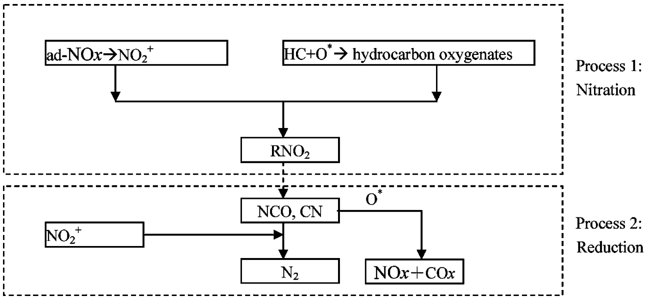

Fig. 15. The essential pathways in thermal SCR over Ag/Al_2O_3.

or fast oxidation of –NCO species under this condition (Fig. 6). High concentration of propene in the reaction gas decreases the amount of active oxygen over Ag/Al_2O_3 and suppresses the oxidation of –NCO species, leading to effective NO_x reduction at high temperatures. When propene was activated in N_2, NO_x conversion was even higher than that in thermal SCR at 550 °C. Since part of –NCO species were directly generated from the oxidation of C_xH_yN species, less surface nitrates were need for the thermal nitration process over Ag/Al_2O_3 and then helped to provide more nitrates in the reduction steps.

Based on the discussion above, our proposals for an effective HC-SCR in wide temperature range were as follows: (1) surface nitrates are active in the full temperature range to provide abundant NO_2^+ easily; (2) electron-rich organic groups (i.e. oxygenates) or C_xH_yN species are effectively generated to promote the nitration process; (3) oxidation of –NCO species is strongly suppressed by appropriately controlling the concentration of oxygen over the catalysts.

5. Conclusions

With the aid of non-thermal plasma to activate the feed gas, various intermediates over Ag/Al_2O_3 were enriched, which helped to understand the mechanism in HC-SCR. The reductions in HC-SCR were classified into the nitration and reduction processes, which generates –NCO species and reduces ad-NO_x, respectively. Abundance of proposed NO_2^+ and electron-rich organic species over Ag/Al_2O_3 were possibly considered to be favorable for the nitration reactions. Activating propene in an O-predominant environment in NTP provides abundant oxygenate species and enhances the efficiency of SCR over Ag/Al_2O_3 by the promotion of the nitration process above 250 °C. Activating propene in a N-predominant environment in NTP to provide $C_xH_yO_zN$ species, which can be oxidized or decomposed to –NCO species directly, is another way to promote the nitration process in HC-SCR. Appropriate amount of NO_2^+ from ad-NO_x may be essential in the process of NO_x reduction. The low efficiency of NTP-assisted C_3H_6-SCR below 250 °C was attributed to the inability of providing enough NO_2^+ from ad-NO_x at low temperatures. The oxidation of –NCO species in the reduction process should be strongly suppressed for an effective reduction of NO_x.

Acknowledgements

The work was financially supported by National Natural Science Fund of China (Grant No. 20677034 and 20437010), and the National High-Tech Research and Development (863) Program of China (Grant No. 2006AA060301), and New Century Excellent Talents in University of China (NCET-2005).

References

[1] M. Iwamoto, H. Yahiro, S. Shundo, Y. Yuu, N. Mizuno, Appl. Catal. 69 (1991) 15–19.
[2] W. Held, A. Konig, R. Thomas, SAE Trans. 99 (1990) 209–216.
[3] J. Li, Y. Zhu, R. Ke, J. Hao, Appl. Catal. B 80 (2008) 201–203.
[4] M. Shelef, R.W. McCabe, Catal. Today 62 (2000) 35–50.
[5] P. Forzatti, Appl. Catal. A 222 (2001) 221–236.
[6] R. Burch, J.P. Breen, F.C. Meunier, Appl. Catal. B 39 (2002) 283–303.
[7] J. Li, J. Hao, L. Fu, T. Zhu, Z. Liu, X. Cui, React. Kinet. Catal. Lett. 80 (2003) 75–80.
[8] Z. Liu, J. Hao, L. Fu, T. Zhu, J. Li, Appl. Catal. B 48 (2004) 37–48.
[9] Z. Liu, J. Hao, L. Fu, T. Zhu, Appl. Catal. B 44 (2003) 355–370.
[10] O. Okada, T. Tabata, M. Kokitsu, H. Ohtsuka, L.M.F. Sabatino, G. Bellussi, Appl. Surf. Sci. 121–122 (1997) 267–272.
[11] J.A. Martens, A. Cauvel, F. Jayat, S. Vergne, E. Jobson, Appl. Catal. B 29 (2001) 299–306.
[12] Z. Liu, J. Hao, L. Fu, J. Li, X. Cui, Sino. Env. Sci. 25 (2004) 7–12.
[13] T. Zhu, J. Hao, L. Fu, X. Cui, Y. Wu, Sino. Env. Sci. 23 (2002) 13–17.
[14] K. Masuda, K. Tsujimura, K. Shinoda, T. Kato, Appl. Catal. B 8 (1996) 33–40.
[15] T. Miyadera, Appl. Catal. B 2 (1993) 199.
[16] N. Bogdanchikova, F.C.M.M. Avalos-Borja, J.P. Breen, A. Pestryakov, Appl. Catal. B 36 (2002) 287–297.
[17] K. Shimizu, J.S.H. Yoshida, A. Satsuma, T. Hattori, Appl. Catal. B 30 (2001) 151–162.
[18] K. Shimizu, A.S.T. Hattori, Appl. Catal. B 25 (2000) 239–247.
[19] K. Eränen, F.K.K. Arve, L. Lindfors, D.Yu. Murzin, J. Catal. 227 (2004) 328–343.
[20] R. Burch, J.P.B.F.C. Meunier, Appl. Catal. B 39 (2002) 283–303.
[21] T. Miyadera, Appl. Catal. B 16 (1998) 155–164.
[22] H. Gao, H. He, Spectrochim. Acta Part A 61 (2005) 1233–1238.
[23] A. Satsuma, K.-I. Shimizu, Prog. Energy Combust. Sci. 29 (2003) 71–84.
[24] Y. Yu, H. He, Q. Feng, H. Gao, X. Yang, Appl. Catal. B 49 (2004) 159–171.
[25] N. Bion, J.S.M. Haneda, M. Daturi, J. Catal. 217 (2003) 47–58.
[26] F.C. Meunier, J.P.B.V. Zuzaniuk, M. Olsson, J.R.H. Ross, J. Catal. 187 (1999) 493–505.
[27] H. Miessner, K.-P. Francke, R. Rudolph, Appl. Catal. B 36 (2002) 53–62.
[28] H. Miessner, K.-P. Francke, R. Rudolph, Th. Hammer, Catal. Today 75 (2002) 325–330.
[29] D.N. Tran, C.L. Aardahl, K.G. Rappe, P.W. Park, C.L. Boyer, Appl. Catal. B 48 (2004) 155–164.
[30] C.L. Aardahl, R.T. Rozmiarek, K.G. Rappe, D.P. Mendoza, P.W. Park, 13th International Congress on Catalysis, Paris, France, July 11–16, 2004.
[31] S. Yoon, A.G. Panov, R.G. Tonkyn, A.C. Ebeling, S.E. Barlow, M.L. Balmer, Catal. Today 72 (2002) 243–250.
[32] S. Yoon, A.G. Panov, R.G. Tonkyn, A.C. Ebeling, S.E. Barlow, M.L. Balmer, Catal. Today 72 (2002) 251–257.
[33] J.H. Kwak, J. Szanyi, C.H.F. Peden, J. Catal. 220 (2003) 291–298.
[34] J.H. Kwak, J. Szanyi, C.H.F. Peden, Catal. Today 89 (2004) 135–141.
[35] R.G. Tonkyn, S.E. Barlow, J.W. Hoard, Appl. Catal. B 40 (2003) 207–217.
[36] K.G. Rappe, J.W. Hoard, C.L. Aardahl, P.W. Park, C.H.F. Peden, D.N. Tran, Catal. Today 89 (2004) 143–150.
[37] A. Gal, M. Kurahashi, M. Kuzumoto, J. Phys. D 32 (1999) 1163–1168.
[38] Z. Chen, V.K. Mathur, Ind. Eng. Chem. Res. 42 (2003) 6682–6687.
[39] M. Dors, J. Mizeraczyk, Catal. Today 89 (2004) 127–133.
[40] Y. Lu, Z. Deng, Applied Infrared Spectral Analysis, Publishing House of Electronics Industry, Beijing, 1989.
[41] K. Shimizu, H. Kawabata, A. Satsuma, T. Hattori, Appl. Catal. B 16 (1998) 319–326.
[42] Y. Yu, H. He, Chin. J. Catal. 24 (2003) 385–390.
[43] Q. Wu, H. He, Y. Yu, Appl. Catal. B 61 (2005) 107–113.
[44] I. Orlandini, U. Riedel, Catal. Today 89 (2004) 83–88.
[45] E.D. Hughes, C.K. Ingold, R.I. Reed, Nature 158 (1946) 448–449.
[46] R. Brosius, K.A.M.H. Groothaert, J.A. Martens, J. Catal. 231 (2005) 344–353.
[47] F.C. Meunier, R.U.C. Stapleton, J.R.H. Ross, Appl. Catal. B 30 (2001) 163–172.
[48] B. Wichterlová, P.S.J.P. Breen, R. Burch, C.J. Hill, L. Čapek, Z. Sobalík, J. Catal. 235 (2005) 195–200.
[49] S. Satokawa, J.S.K. Shimizu, A. Satsuma, T. Hattori, Appl. Catal. B 42 (2003) 179–186.
[50] M. Nguye, A.F. Hegarty, J. Chem. Soc., Perkin Trans. II (1984) 2043–2045.
[51] K. Shimizu, M. Hashimoto, J. Shibata, T. Hattori, A. Satsuma, The 2nd Japan-China Workshop on Environmental Catalysis and Eco-materials, Fukuoka, Japan, October 23–25, 2005.
[52] M. Haneda, Y.K.H. Hamada, Appl. Catal. B 20 (1999) 289–300.